Shape Complexity and Process Energy Consumption in Electron Beam Melting

A Case of Something for Nothing in Additive Manufacturing?

Martin Baumers, Chris Tuck, Ricky Wildman, Ian Ashcroft, and Richard Hague

Keywords:

3D Printing
additive manufacturing (AM)
electron beam melting (EBM)
energy consumption
industrial ecology
shape complexity

Supporting information is available on the *JIE* Web site

Summary

Additive manufacturing (AM) technology is capable of building up component geometry in a layer-by-layer process, entirely without tools, molds, or dies. One advantage of the approach is that it is capable of efficiently creating complex product geometry. Using experimental data collected during the manufacture of a titanium test part on a variant of AM technology, electron beam melting (EBM), this research studies the effect of a variation in product shape complexity on process energy consumption. This is done by applying a computationally quantifiable convexity-based characteristic associated with shape complexity to the test part and correlating this quantity with per-layer process energy consumption on the EBM system. Only a weak correlation is found between the complexity metric and energy consumption ($\rho = .35$), suggesting that process energy consumption is indeed not driven by shape complexity. This result is discussed in the context of the energy consumption of computer-controlled machining technology, which forms an important substitute to EBM. This article further discusses the impact of available additional shape complexity at the manufacturing process level on the incentives toward minimization of energy inputs, additional benefits arising later within the product's life cycle, and its implications for value creation possibilities.

Introduction

Researchers argue that action is needed to limit anthropogenic climate change; it is claimed that humanity's ecological footprint already far exceeds earth's capacity (Westkämper et al. 2000; Jovane et al. 2008). Moreover, an understanding of the emissions associated with manufacturing processes is essential regarding decision making toward sustainability. In particular, the measurement of carbon emissions, known as "carbon accounting," requires a fundamental understanding of the energy flows associated with production processes (Vijayaraghavan and Dornfeld 2010).

Marked by ongoing technological development, additive manufacturing (AM) is a relatively recent manufacturing approach, with various technology variants being introduced during the 1980s and 1990s (Kruth et al. 1998; Levy et al. 2003). The ASTM (2012, 2) defines AM processes as being capable of "joining materials to make objects from 3D model data, usually layer upon layer, as opposed to subtractive manufacturing methodologies." This article assesses the energy consumption characteristics of one particular AM technology variant, electron beam melting (EBM).

The general operating principle of EBM and the main system components are described in figure 1. An electron beam is emitted by a filament and sequentially passes through focus coils controlling spot size and deflection coils controlling beam direction, all of which are located within a beam column (a). The focused electron beam selectively melts the surface of a

Address correspondence to: Martin Baumers, 3D Printing Research Group, Faculty of Engineering, University of Nottingham, Nottingham NG7 2RD, United Kingdom. *Email*: martin.baumers@nottingham.ac.uk; *Web*: www.nottingham.ac.uk/3dprg

DOI: 10.1111/jiec.12397

Editor managing review: Michael Hauschild

Volume 00, Number 0

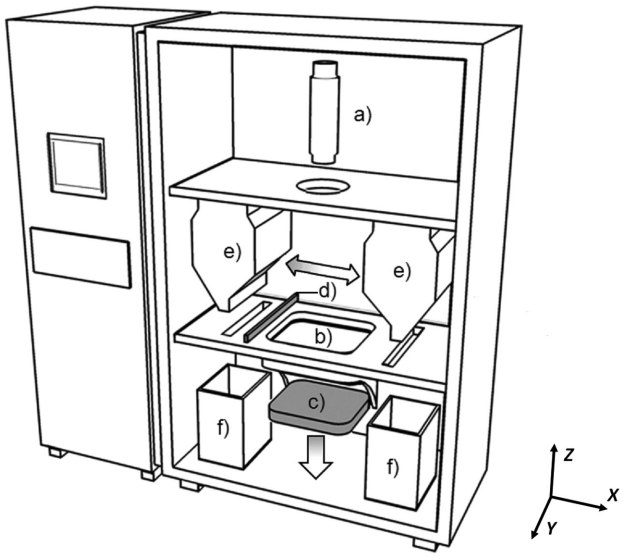

Figure 1 Main components of an EBM system: (a) beam column, (b) powder bed, (c) build platform, (d) powder rake, (e) powder hoppers, and (f) overflow bins. EBM = electron beam melting.

Table 1 Arcam A1 system characteristics, as employed for this research

System type	*Arcam A1*
Beam type	Electron beam
Maximum beam energy	3,000 W
Nominal build volume size (X/Y/Z)	200/200/180 mm
Measured usable platform area (X/Y)	180/180 mm
Investigated build material	Titanium, Ti-6Al-4V, grade 5 (ASTM 2013)
Layer thickness	70 μm
Process atmosphere	Vacuum, with addition of He
Powder bed temperature	~700ºC
Power supply	400 V, 16A, multiphase
Chiller on external power	No
Manufacturer reference	Arcam AB (2014)

Note: W = watts; mm = millimeters; μm = micrometers; V = volts.

powder bed (b) layer by layer. After completing each layer with a fixed layer height of 70 micrometers (μm), the build platform (c) moves down by an increment in the vertical ("Z") direction and a "powder rake" (d) deposits a fresh layer of metal powder in the horizontal ("X") direction, dispensed from stationary powder hoppers (e). The rake also discards any excess powder into overflow bins (f) for reuse. This cycle repeats until the build is complete. After completion of all layers, the build platform (c) holding the products is removed. Table 1 summarizes important characteristics of the investigated A1 EBM machine.

For details on EBM's operating principle, see Hopkinson and Dickens (2006), Heinl and colleagues (2007), or Murr and colleagues (2009). EBM platforms have been judged to be particularly energy efficient variants of AM (Taminger and Hafley 2002; Heinl et al. 2007; Frigola et al. 2008). Strutt (1980) points out that energy transfer by the electron beam principle is around 10 times more efficient than by laser beam, which is the approach employed by most other metallic AM technology variants. An investigation of the microstructural and mechanical properties achievable by EBM, including the thermal effects of the process, is provided by Al-Bermani and colleagues (2010).

It is suggested that AM technology has two generic advantages over other manufacturing processes (Tuck et al. 2008). First, AM allows the manufacture of designs without many of the geometric constraints limiting the complexity of shapes that are associated with other processes and treated in the literature on design for manufacturability (Boothroyd et al. 1994; Bralla 1998). Second, AM enables the manufacture of customized products in small volumes at a relatively low average cost. The current state of AM technology, however, also carries a set of generic process limitations (Ruffo and Hague, 2007), acting as a barrier to the adoption of AM process in several applications:

- limited material selection and characteristics,
- low process productivity,
- low dimensional accuracy,
- rough surface finish,
- repeatability and quality issues, and
- relatively high unit cost at medium and large volumes.

In the context of monetary production cost, it has been suggested that AM allows the manufacture of more complex product geometry at no additional cost (Hague et al. 2003). Taking a step beyond financial cost, this article is interested in whether extra shape complexity is also available at no additional process energy consumption, which may result in additional use-phase performance advantages for applications that benefit from complex design.

Shape complexity factors are used to determine efficient manufacturing process configurations, for example, in forging or machining processes. A basic measure used in this context is the Spies ratio S (Spies 1957), which is calculated by dividing a part's mass m_{part} over the mass of a correctly aligned bounding primitive $m_{primitve}$, typically a cylinder or a cuboid, made of the same material. Building on this concept, Tomov and Radev (2007) report a selection of shape complexity factors designed to enable the specification of an efficient sequence of forging steps by estimating the work needed for material deformation during the forging process. Similarly, Kerbrat and colleagues (2010) develop a set of manufacturing complexity indices applicable to computer numerically controlled (CNC) machining and AM in order to inform process selection and design modularization approaches for improved manufacturability and lower cost.

However, the methodology used in this paper is based on the assumption that using such a primarily process-flavored approach to the measurement of complexity does not provide a suitable pathway for the investigation of marginal effects of changes of shape complexity. The reason for this is that if manufacturing process characteristics are present in the formulation of the complexity metric it is difficult to identify any changes of process characteristics, such as energy consumption, in response to changes in shape complexity. Therefore, this paper

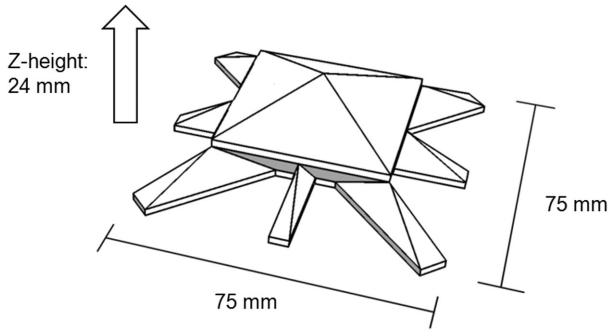

Figure 2 Spider-shaped test part geometry. Image source: Baumers (2012).

views shape complexity as a characteristic derived from the geometry manufactured, implicitly accommodating aspects of the processes, rather than deriving from the processes used to generate them. Reporting the results of previous doctoral research (Baumers 2012), this research thus correlates process energy consumption to characteristics associated with geometric complexity.

The following part of this paper, *Methods and Implementation*, outlines the methodology employed in the construction of an algorithm designed to capture shape complexity and presents the experimental setup used to collect power consumption data. *Results* presents the measured variation in the investigated test part and per-layer energy consumption results. The *Discussion* section examines these results in the context of CNC machining, which forms an important substitute manufacturing technology, and seeks to extract further meaning by relating the results to a selection of concepts from the literature on industrial energy consumption reduction and on benefits arising from the availability of additional complexity within high-technology industries. The final section, *Conclusion*, provides a summary and makes recommendations for further research.

Methods and Implementation

To facilitate this investigation, it was decided to base power monitoring experiments on a test part geometry, as done by Mognol and colleagues (2006). The layer-by-layer operating principle of EBM allows the design of a power monitoring geometry tailored for the analysis of the impact of geometric variables on energy consumption by varying the part's cross-section along the vertical ("Z") direction. The resulting test part, shown in figure 2, exhibits a suitable variation in two parameters, shape complexity and cross-sectional area, as will be explored in the following sections.

The part's lower half is designed to assess the effect of shape complexity on energy inputs. This is done by changing a complex, star-shaped cross-section with a square cutout in the center into a square cross-section (at 12 millimeters [mm] Z-height). In the upper half of the geometry, the effect of cross-sectional area, reflective of overall part size, is explored. This is achieved by simply reducing cross-section area A down to a value of zero, forming a single vertex in a pyramid-like upper tip. A further point of consideration in the design of the "spider" shape shown in figure 2 was that some areas of the geometry feature negative wall angles. To avoid the use of support structures in the build experiments on the EBM system, the part was designed to not exceed negative wall angles of 45º.

Implementing a Complexity Measurement Algorithm

Complexity forms an inherently multifaceted concept (Edmonds 1999) that may relate to, among other things, the logical depth or the difficulty of identifying original patterns (Gell-Mann 1995), or the number of nodes and connections in a network structure (Gilder 1989). Regarding the measurement of the complexity of real-world objects such as manufactured products, it has been argued that a narrow view on the quantities relating to such complexity may be unavoidable, making such metrics depend on the context (Gell-Mann 1995).

An algorithmic approach suitable for this article was developed by Psarra and Grajewski (2001), associating the measurement of two-dimensional (2D) shape complexity with various convexity-based classes of regularity. This technique was designed with the original intent of computationally assessing floor plans in architecture.

In an adapted form, and combined with an implementation inspired by radar systems, this article develops the technique to be able to quantify shape features associated with complexity in the test part shown in figure 2 (and indeed any other part). This approach is particularly useful because it is able to capture aspects associated with both the topological and geometrical aspects of shape complexity. Transferring the technique to the analysis of three-dimensional (3D) solid object geometry, the special layer-by-layer operating principle of AM allows the underlying 2D method to be maintained. This is possible because current additive equipment, such as the analyzed EBM platform, operates in a strictly sequential manner completing each horizontal layer before depositing the next layer onto the existing geometry. Thus, AM permits a separate analysis of every 2D cross-section.

By subjecting the cross-section of a test part to a controlled variation along the test part's Z-axis, this research extends the original algorithmic approach by Psarra and Grajewski (2001). Effectively, a continuous 3D solid is split into a sequence of 2D layers, so that the level of shape complexity can be varied within one build. The effect of the variation of shape complexity on process energy consumption of AM can then be studied.

The first step toward the computational approach is, of course, a discretization process. The complexity measurement algorithm is based on a manually discretized version of the test part shown in figure 2, which is hard coded in a 3D array. Corresponding to the discretization resolution in $(1\ \text{mm})^3$ volumetric pixels ("voxels"), the variation of shape complexity is measured in 1-mm intervals of Z-height. This resolution was chosen to balance the computational power needed for this approach (written in C++) with sufficient accuracy.

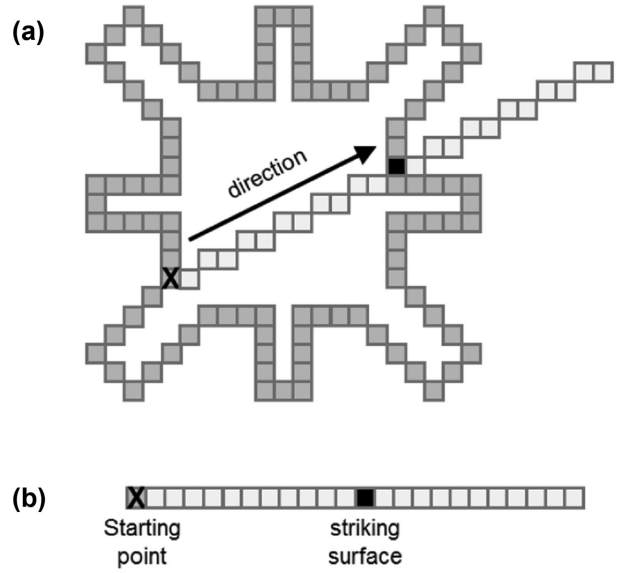

Figure 3 Implementation of occlusion measurement: (a) top view on a discretized layer (voxel resolution and scale not accurate) and (b) illustration of a one-dimensional array for the determination of visible voxels. Image source: Baumers (2012).

Once the specifically designed power monitoring geometry is discretized, the next step is to develop an algorithm that is designed to assess each discrete voxel element of the part's surface for complexity in a succession of horizontal cross-sections (analogous to build layers). Expressed intuitively, the proportion of other surface elements that are directly visible from specific loci in a layer can thus be identified. The outcome of this calculation is a mean connectivity value (*MCV*) characterizing the shape complexity of each horizontal slice of the test part. Mimicking the layer-by-layer principle of AM, the resulting algorithm assesses each layer separately, resulting in a series of *MCV* values for each horizontal layer of the discretized test geometry.

The actual algorithm underlying the measurement of such "visibility" is inspired by radar systems used to measure the distance of surrounding objects relative to a location. Radar systems operate by emitting signals in predetermined directions, often using antennae rotating around a Z-axis. A Cartesian coordinate system is used in the implementation, which may deviate from the original inspiration of radar. The principle of the measurement algorithm is very similar, however. Starting with the first element of the perimeter of the initial layer under consideration, a "radar signal" is emitted. Once the signal has been sent, it travels through the discretized voxel space in the predetermined direction. Where it strikes another element of the surface, the location is recorded. If it does not strike the perimeter at any location, for example, if it is emitted toward the outside of the shape, no impact location is registered.

This radar-inspired implementation works as follows: As illustrated in figure 3a, the algorithm reads discretized information on part geometry in a particular direction, recording the content of the voxel cells approximating the part in a one-dimensional (1D) array (figure 3b). In this sequence, beginning from the starting point, each entry is interrogated for a surface hit. The location of the first cell struck in this sequence is then recorded in a further array.

The direction, or gradient, of the "radar beam" is then changed by one increment in counterclockwise direction and new information is read into the 1D array (figure 3b). This is repeated in a loop, until the full 360º circle is complete around the starting point and all visible cells have been recorded. In the following step, the algorithm compares the location of the recorded visible elements to what should be visible without occlusion.

If every existing surface element is visible, the shape is deemed fully convex, as proposed by Psarra and Grajewski (2001). For intermediate results, a value of connectivity $CV \in]0, 1]$ will be the result. This procedure is repeated for all "*n*" elements of the perimeter in layer "*i*", enabling the calculation of the mean connectivity value MCV_i for each layer, where (equation 1):

$$MCV_i = \frac{\sum_{m=1}^{n} CV_m}{n} \quad (1)$$

MCV is calculated for all layers in the discretized approximation of the test part. Effectively, MCV_i reflects shape complexity present in the "*i*"th horizontal cross-section of the part and thus forms a measure of 2D shape complexity. The measurement algorithm is available in the form of pseudocode in the Supporting Information available on the Journal's website.

Power Monitoring Experiments

To assess the effect of a variation in part geometry on the energy consumed to deposit a layer, a build experiment has been performed on the Arcam A1 EBM system. Acknowledging that AM systems of this type only operate efficiently if the available build capacity is utilized (Baumers et al. 2011), a batch of five power monitoring test parts was produced in a full build experiment. As required by the methodology, all test parts were built in the same orientation directly onto the removable build plate, without any connecting or support structures.

The electricity consumption during the build experiments was recorded using a Yokogawa CW240 digital multipurpose power meter (Yokogawa Electric Corp. 2004), the main variable of interest being mean real power consumption across the three phases and the neutral line. To assemble the required data set, it is necessary to synchronize the collected energy consumption data with the log files created by the A1's operating system, providing information on machine state and build progress. This information is extracted from the build log files in the *.plg file format using Arcam's LogStudio tool (v.3.1.51).

Results

Cross-sectional shape complexity is quantified by calculating a metric of shape complexity, which is the mean value of "visibility," MCV_i, for each layer "*i*", as shown in equation (1).

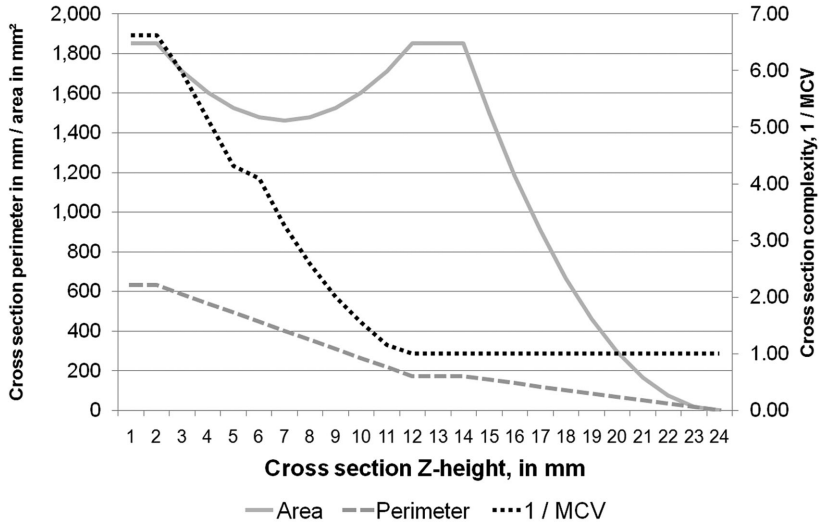

Figure 4 Variation of parameters of geometry. Image source: Baumers (2012).

Because the implementation of the measurement algorithm is based on a resolution of (1 mm)³ voxels, the corresponding variation of test part parameters is measured in 1-mm intervals of Z-height. Figure 4 shows the variation of three parameters along the test part's Z-axis: the total area of the part's cross-section; the cross-sectional perimeter length; and the parameter of shape complexity. For exposition, MCV is shown in inverted form, such that a high value of MCV^{-1} indicates high cross-sectional shape complexity.

As figure 4 demonstrates, the area of the cross-sections dips between 2 and 12 mm of Z-height, from an initial value of 1,850 square millimeters (mm²) to around 1,450 mm². This fluctuation occurs alongside the controlled variation of MCV. The fact that both parameters are varied in parallel complicates the analysis of the pure effect of a variation of MCV. However, it does allow the design of a relatively simple polygonal test part without curved surfaces, as shown in figure 2. The irregularity in the MCV^{-1} curve at a Z-height of 6 mm results from the use of a discretized voxel representation of part geometry. It is thus an artefact of the discretization technique and should be ignored.

It has been argued that for any measure of complexity to be useful, at least one of the surveyed features must exhibit high complexity (Gell-Mann 1995). Figure 4 demonstrates that the design of a test part jointly varying parameters of complexity and cross-sectional area is successful by this standard. The effect of these variations of area and complexity along the Z-axis can now be explored in terms of the per-layer process energy consumption data.

Power Monitoring Results

Build operations on an EBM platform consist of four phases: system startup; preheating; build phase; and machine cool-down. The energy consumption results are reported in table 2, listing process time, mean real power consumption, and cumulative energy consumption during the various phases of the build. This results in a specific energy consumption of 59.96 megajoules (MJ) per kilogram (kg) deposited, which corresponds to the energy consumption results reported for other AM technology variants (Mognol et al. 2006; Kellens et al. 2010; Le Bourhis et al. 2013). It should be noted that the power consumed by the platform's internal chiller is included in the measurement.

By combining the energy consumption data with the information retrieved from the machine's log file, it is possible to divide the energy invested during the core build time into three machine activities: (1) layer preparation; (2) layer preheating; and (3) melting.

Figure 5 shows that the energy expended during layer preparation (data loading and fresh powder deposition by the powder deposition mechanism shown in figure 1d) fluctuates around a constant mean throughout the build (approximately 10 kilojoules per layer). In contrast, the energy expended during the preheating state exhibits a linear, slightly negative, trend—most likely owing to a gradual warming up of the machine frame during the build process, decreasing the requirement for energy expenditure for layer preheating over time. More interestingly, the energy expended for the selective melting of the cross-sections fluctuates strongly. The initial spike in energy consumption (during the first layer) is explained by repeat melting to ensure full attachment of parts to the build platform.

Correlation between Complexity and Energy

Visual inspection of figure 5 suggests that the observed pattern of energy expenditure for melting (dashed line) can be explained by cross-sectional area. The Pearson product-moment correlation coefficient $\rho_{X,Y,}$ where (equation 2):

$$\rho_{X,Y} = \frac{cov\,(X, Y)}{\sigma_X \sigma_Y}\,, \qquad (2)$$

Table 2 EBM power monitoring results

Category	*Characteristic*	*Value*
Process time	Warm-up time: machine startup	10 min
	Warm-up time: preheating	14 min
	Build time	260 min
	Cool-down time	17 min
	Total build time	**301 min**
Power consumption	Mean real power consumed: machine startup	1.09 kW
	Mean real power consumed: preheating	3.90 kW
	Mean real power consumed: build	2.22 kW
	Mean real power consumed: cool-down	0.60 kW
	Mean real power consumed, overall	**2.17 kW**
Absolute energy consumption	Energy consumption: machine startup	0.62 MJ
	Energy consumption: preheating	3.27 MJ
	Energy consumption: build time	34.66 MJ
	Energy consumption: cool-down	0.61 MJ
	Total energy consumption	**39.16 MJ**
Specific energy consumption	**Energy consumed per part (5 in total)**	**7.83 MJ**
	Energy consumed per cm³ deposited	**0.27 MJ**
	Specific energy consumption per kg deposited[a]	**59.96 MJ**

[a]Assuming 100% part density, at 4.43 g/cm^3.
EBM = electron beam melting; cm^3 = cubic centimeters; kg = kilogram; min = minutes; kW = kilowatts; MJ = megajoules; g/cm^3 = grams per cubic centimeter.

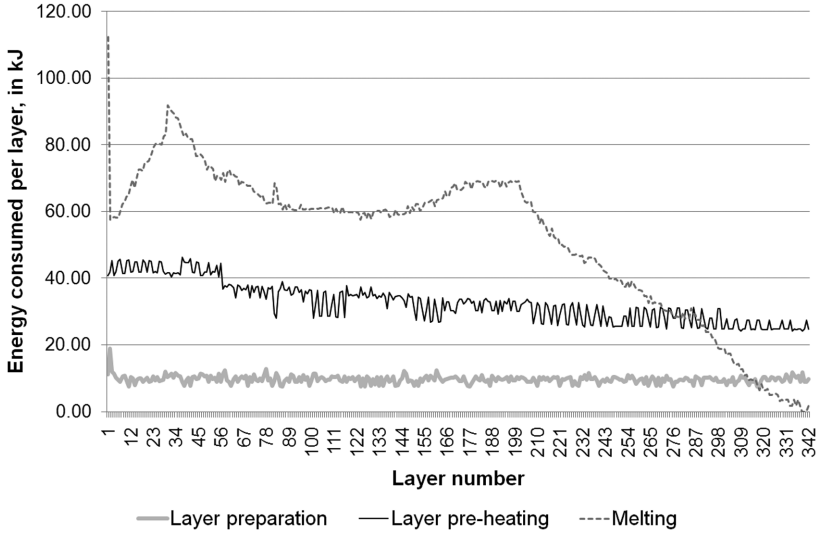

Figure 5 EBM energy invested per layer, by activity. Image source: Baumers (2012). EBM = electron beam melting.

and $\sigma_X\sigma_Y$ is the product of the standard deviations of variables X and Y, can be used to express the degree of linear dependence between two variables. A sample correlation coefficient $\rho_{Area,Layer\ Energy} = 0.9699$ between selective melting energy and cross-sectional area (in 1-mm intervals of Z-height) suggests that total melting energy consumption is indeed determined by cross-sectional area and thus by overall part mass.

Further applying correlation coefficients, the effects of various aspects of geometry on the energy expended for layer melting can be studied. Focusing on the portion of the build containing variation of shape complexity (1 to 12 mm Z-height, as shown in figure 2), correlation coefficients between layer energy and cross-sectional perimeter length, complexity, and melting area can be compared (equations 3, 4, and 5):

$$\rho_{Perimeter,\ Layer\ Energy} = 0.6568 \quad (3)$$

$$\rho_{Area,\ Layer\ Energy} = 0.8263 \quad (4)$$

$$\rho_{MCV,\ Layer\ Energy} = -0.3544 \quad (5)$$

The coefficients demonstrate that melting energy consumption correlates strongly with cross-section area (0.8263) and, to a lesser extent, with perimeter length (0.6568). The correlation coefficient between layer energy consumption and the used measure of shape complexity (–0.3544) is small. This can be viewed as evidence of a weak or potentially absent association between EBM energy consumption and cross-sectional shape complexity. It should be noted that the negative correlation coefficient originates from the formulation of MCV_i (a high value indicates a small degree of shape complexity and vice versa).

This article acknowledges that the test part geometry, shown in figure 2, was selected to avoid the requirement to deposit support structures. This is, of course, a simplification that routinely does not hold in reality and must flow into the consideration of the calculated correlation coefficients. On the other hand, there is an incentive to minimize the use of such structures and their volume to reduce part finishing and cost (Cloots et al. 2013).

Discussion

The experimental results presented in this article suggest that EBM does not exhibit a strong direct linkage between energy consumption and shape complexity, at least on a per-layer basis. Therefore, this article argues that there is no clear connection between the feature richness of a component and the energy needed to deposit it by EBM. Rather, it appears that process energy consumption is driven by cross-sectional area and hence by overall part mass.

It should be remarked at this point that the used test geometry, featuring a controlled variation along the Z-axis, may resemble a relatively noncomplex component, especially when compared to some applications of EBM incorporating internal or external lattice structures (see, e.g., Murr et al. 2012). Thus, a higher degree of realism could be achieved by incorporating such structures into the analysis. Further, the test specimen does not necessitate expendable support structures, which are routinely required in the EBM process. A support-free design was specified to allow an investigation of the effects of 2D cross-sectional shape complexity; this approach would not have been possible in the presence of auxiliary structures.

Moreover, this analysis forms an investigation of energy consumption at the process level. It thus does not investigate the environmental impact occurring during other stages in the product life cycle. Especially for the manufacturing of titanium materials, the associated environmental impacts have been documented as significant (Granta Design 2010). The production of virgin Ti-6Al-4V cast material is estimated to consume from 582 to 643 MJ/kg. Because titanium is seldom manufactured purely from precursor materials, it is also necessary to consider the energy embodied in recycled material, between 221 and 244 MJ/kg, and a recycling rate of between 20.9% and 23.1%. Using the mean values of these data points (all provided by Granta Design [2010]), this research assumes a total embedded energy of 528.90 MJ/kg for Ti-6Al-4V plate material. To convert this material into the required powderous form (spherical particles with 15 to 45 μm diameter), a gas atomization route can be employed. The energy consumed for this additional process has been estimated from 30.1 to 33.3 MJ/kg processed (Granta Design 2010). Again using the mean of these two data points, the total energy requirement to create Ti-6Al-4V powder can be approximated at 560.60 MJ/kg, representing an additional energy investment of only 6% compared to plate material.

Additionally, this research notes that EBM platforms also consume helium to maintain a controlled vacuum and for process cool-down. The equipment manufacturer cites a helium consumption rate of 1 liters per hour (L/h) and a cool-down helium consumption of 50 to 75 L per build for the successor system to the investigated A1 platform (Arcam 2014). In terms of volume, this flow is far lower than the nitrogen consumption (3,500 L/h) observed by Kellens and colleagues (2010) for a laser-based powder bed fusion platform.

By concentrating on the core process level, this research ignores aspects of postprocessing. Such postprocessing for EBM products can be performed by light finish machining (Cormier et al. 2004) or shot blasting (Mazzioli et al. 2009). This research acknowledges that the additional energy consumption required to postprocess products may be related to the shape complexity exhibited by designs, dependent on the used technique. Further, Baumers and colleagues (2013) report the requirement for a wire erosion process to separate parts from the build platform for a laser-based powder bed fusion system, estimating a fixed energy consumption of 142.46 MJ. The investigated EBM platform does not require a separation process because the manufactured parts were hand-separable from the platform owing to differences in thermal expansion of the build material (Ti-6Al-4V) and the steel build platform.

As a first point of discussion, the results presented by this article can be contrasted with empirical data from machining processes. In the production of small, geometrically complex or customized parts, EBM has been adopted in place of CNC machining processes (Harryson et al. 2005; Morrow et al. 2007). Morrow and colleagues (2007) show how consecutive CNC operations increase the energy invested into a part. As can be seen from figure 6, the energy consumed by the various steps is highly nonuniform. This may be because of discrepancies in rough versus finish milling (Morrow et al. 2007) or to variations in the specific energy consumption per unit of material removed (Avram and Xirouchakis 2011). The end result is the same: Overall CNC energy consumption is the outcome of a sequence of manufacturing steps removing raw material and thereby manipulating raw material in billet or bar form into a more complex final product.

As noted above, this analysis of the energy inputs to EBM does not consider the energy embedded in the raw material. Given that CNC machining operations routinely result in significant waste streams in the form of machining swarf and EBM will result in little (if any) process-related raw material wastage, a substantial additional energy saving may be available through the adoption of EBM.

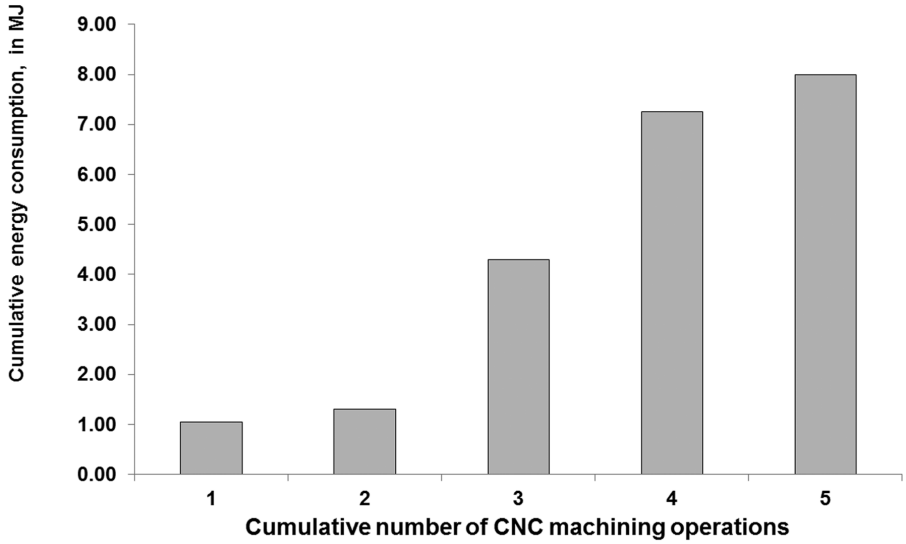

Figure 6 Cumulative energy consumption in MJ, by CNC operation. Image source: adapted from Morrow and colleagues (2007). MJ = megajoules; CNC = computer numerically controlled.

Unlike machining processes, the results presented in this article show that a minimization of deposited volume can be expected to lead to a minimization of process energy consumption in EBM. An important linking argument is the assumption that process energy consumption and production cost correlate positively, which has been observed for the AM process variant, direct metal laser sintering (Baumers et al. 2013), which is closely related to EBM. This implies that cost minimization by the technology operator should coincide with the minimization of process energy consumption.

The described relationship produces a situation of correctly aligned incentives: The private incentive of cost minimization will motivate the deposition of the smallest possible amount of material, which, in turn, will result in the smallest amount of process energy consumption. Such an alignment of the private cost minimization incentive with configurations minimizing energy consumption, and hence a significant external environmental footprint, has been classed as an important prerequisite for the reduction of energy inputs (Lovins 1996).

Further, where the deposited volume can be reduced while maintaining part performance through an increase in shape complexity, a range of possible financial and environmental savings may follow during the use phase, especially in weight-sensitive applications (Helms and Lambrecht 2007). Thus, this article argues that cost minimization is likely to inadvertently lead to virtuous knock-on effects: By minimizing energy consumption during the manufacturing stage of applications in which component mass plays a role for product performance, end-use efficiency may also be improved. This results in lower operating costs (see, e.g., Kaufmann 2008) and lower environmental impacts associated with, for example, reduced fractional fuel consumption (Economon et al. 2011). Further savings may be enabled through secondary mass reductions that become possible through the lightweighting of structural or other components (Saidpour 2004).

Moreover, the results presented in this article suggest that geometry and functional features can be added at low or even negligible additional process energy consumption if they do not coincide with increases in deposition volume. This point is closely related to phenomena normally associated with technological progress in the manufacturing of microelectronics. In this sector, the near costless availability of additional functional features, mainly logical elements created by planar photolithographic processes, has had a tremendous effect on the performance of electronics over the past decades (Gilder 1989; Schaller 1997; Brynjolfsson and McAfee 2014). This reality of creating extra functional value and utility out of an increased ability to harness complexity in manufacturing processes has been labeled "ex nihilo" value creation (Graeber 2012). The same argument has been extended to the manufacture of computer networking technology (Gilder 2000).

Effectively, the observations made in this article demonstrate that, on the manufacturing process level, there is not necessarily a connection between the utility of the stream of services available from a durable good (for a discussion of the stream of services, see, e.g., Waldman [2003]) and the energy expended to create it. The presented results should therefore be treated as an indication that "value ex nihilo" phenomena may also be approximated within manufacturing processes for parts performing a structural or mechanical function, promising significant environmental benefits.

Conclusion

This article has discussed the evidence for EBM's weak connection between extra product shape complexity and increasing per-layer manufacturing energy requirements. It has shown that

cross-sectional melting area must be viewed as the determinant of energy consumption per layer. This result lends support to the position that process energy consumption is only weakly related, if at all, to the design features and the functional richness of the product. In its discussion of these results, this article has identified three consequences:

1. It is expected that the connection between the minimization of volume and the minimization of process energy consumption will incentivize technology adopters to select minimum energy consumption configurations while choosing a minimum cost configuration.
2. The minimization of deposited volume in conjunction with the exploitation of cheap complexity is expected to lead to improved use-phase performance in weight-sensitive applications. It must be expected that this aspect enables environmental benefits during products' service lives compared to processes exhibiting a clear connection between shape complexity and cost.
3. The result that additional geometry and functional features can be added incurring low additional process energy consumption is likely to allow the creation of significant additional value without large increases of the environmental burden of manufacturing. There are thus grounds to speculate that the use-phase benefits arising from such design changes outweigh their manufacturing process impact.

As the second point emphasizes, the external impact of an ability to efficiently build complex components clearly extends beyond the manufacturing stage of the part's life cycle. Despite efforts to include environmental and social considerations in engineering decisions (Maxwell and van der Vorst 2003), private costs and benefits (accruing to individuals and organizations, as opposed to society) are normally viewed as the determinants of technology adoption decisions (Stoneman 2002). It will therefore be necessary to assess the life cycle of AM products in detail. This will allow research to bridge the gap from manufacturing considerations in isolation to informed statements on the use-phase impact of durable goods, and hence build the case for the environmental savings that may arise overall from the adoption of digital manufacturing technologies such as AM.

Because this research has investigated the manufacture of titanium parts on the technology variant EBM, a further research requirement is to assess how the results presented in this article can be extended and generalized. This is achievable by applying a developed version of this article's experimental setup to a multipart and -platform approach, utilizing a 3D version of the proposed complexity metric to assess different manufacturing pathways. These should include alternative AM processes, such as selective laser melting, as well as conventional substitute techniques, including assembly, bonding, and casting.

References

Al-Bermani, S. S., M. L. Blackmore, W. Zhang, and I. Todd. 2010. The origin of microstructural diversity, texture, and mechanical properties in electron beam melted Ti-6Al-4V. *Metallurgical and Materials Transactions* A 41(A): 3422–3434.

ASTM. 2012. *ASTM F2792-12e1 standard terminology for additive manufacturing technologies*. West Conshohocken, PA, USA: ASTM.

ASTM. 2013. *ASTM B988-13, standard specification for powder metallurgy (PM) titanium and titanium alloy structural components*. West Conshohocken, PA, USA: ASTM.

Arcam, A. B. 2014. Corporate website. www.arcam.com. Accessed 22 December 2014.

Avram, O. I. and P. Xirouchakis. 2011. Evaluating the use phase energy requirements of a machine tool system. *Journal of Cleaner Production* 19(6–7): 699–711.

Baumers, M. 2012. Economic aspects of additive manufacturing: Benefits, costs and energy consumption. Ph.D. thesis, Loughborough University, Loughborough, United Kingdom.

Baumers, M., C. Tuck, R. Wildman, I. Ashcroft, and R. Hague. 2011. Energy inputs to additive manufacturing: Does capacity utilization matter? In Solid Freeform Fabrication (SFF) Symposium, 6–8 August, Austin, TX, USA.

Baumers, M., C. Tuck, R. Wildman, I. Ashcroft, E. Rosamond, and R. Hague. 2013. Transparency built-in. *Journal of Industrial Ecology* 17(3): 418–431.

Boothroyd, G., P. Dewhurst, and W. Knight. 1994. *Product design for manufacture and assembly*. New York: Marcel Dekker.

Bralla, J. 1998. General design principles for manufacturability. In *Design for manufacturability handbook*, edited by J. Bralla. New York: McGraw-Hill.

Brynjolfsson, E. and A. McAfee. 2014. *The second machine age*. New York: W. W. Norton & Company.

Cloots, M., A. B. Spierings, and K. Wegener. 2013. Assessing new support minimizing strategies for the additive manufacturing technology SLM. In Solid Freeform Fabrication (SFF) Symposium, 12–14 August, Austin, TX, USA.

Cormier, D., O. Harryson, and H. West. 2004. Characterization of H13 steel produced via electron beam melting. *Rapid Prototyping Journal* 10(1): 35–41.

Economon, T. D., S. R. Copeland, J. J. Alonso, M. Zeinali, and D. Rutherford. 2011. Design and optimization of future aircraft for assessing the fuel burn trends of commercial aviation. In 49th AIAA Aerospace Sciences Meeting, 4–7 January, Orlando, FL, USA.

Edmonds, B. 1999. What is complexity?—The philosophy of complexity per se with application to some examples in evolution. In *The evolution of complexity*, edited by F. Heylighen and D. Aerts. Dordrecht, the Netherlands: Kluwer.

Frigola, P., R. Agustsson, S. Boucher, A. Murokh, J. Rosenzweig, G. Travish, L. Faillace, D. Cormier, and T. A. Mahale. 2008. Novel fabrication technique for the production of RF photoinjectors. In Proceedings of EPAC08, 13–27 June, Genoa, Italy.

Gell-Mann, M. 1995. What is complexity? *Complexity* 1(1): 16–19.

Gilder, G. F. 1989. *Microcosm: The quantum revolution in economics and technology*. New York: Simon and Schuster.

Gilder, G. F. 2000. *Telecosm: The world after bandwidth abundance*. New York: Simon and Schuster.

Graeber, D. 2012. Of flying cars and the declining rate of profit. In *The baffler 19*. New York: The Baffler and MIT Press.

Granta Design Ltd. 2010. CES EduPack version 6.2.0, 2010. www.grantadesign.com/products/ces/. Accessed 20 February 2011.

Hague, R., I. Campbell, and P. Dickens. 2003. Implications on design of rapid manufacturing. *Proceedings of IMechE Part C: Journal of Mechanical Engineering Science* 217: 25–30.

Harrysson, O., B. Deaton, J. Bardin, H. West, O. Cansizoglu, D. Cormier, and D. Marcellin-Little. 2005. Evaluation of titanium Implant components directly fabricated through electron beam melting technology. In *Medical device materials III—Proceedings of the materials & processes for medical devices conference*. Novelty, OH, USA: ASM International.

Heinl, P., A. Rottmair, C. Körner, and R. F. Singer. 2007. Cellular titanium by selective electron beam melting. *Advanced Engineering Materials* 9(5): 360–364.

Helms, H. and U. Lambrecht. 2007. The potential contribution of light-weighting to reduce transport energy consumption. *The International Journal of Life Cycle Assessment* (special issue) 12(1): 1–7.

Hopkinson, N. and P. M. Dickens. 2006. Emerging rapid manufacturing processes. In *Rapid manufacturing—An industrial revolution for the digital age*, edited by N. Hopkinson, R. J. M. Hague, and P. M. Dickens. Chichester, UK: Wiley.

Jovane, F., H. Yoshikawa, L. Alting, C. R. Boër, E. Westkämper, D. Williams, M. Tseng, G. Seliger, and A. M. Paci. 2008. The incoming global technological and industrial revolution towards competitive sustainable manufacturing. *CIRP Annals—Manufacturing Technology* 57(2): 641–659.

Kaufmann, M. 2008. Cost/weight optimization of aircraft structures. Licentiate thesis, KTH Engineering Sciences, Stockholm, Sweden.

Kellens, K., E. Yasa, W. Dewulf, and J. R. Duflou. 2010. Environmental assessment of selective laser melting and selective laser sintering. Paper presented at Going Green—CARE INNOVATION 2010: From Legal Compliance to Energy-efficient Products and Services, 8–11 November, Vienna.

Kerbrat, O., P. Mognol, and J.-Y. Hascoet. 2010. Manufacturing complexity evaluation at the design stage for both machining and layered manufacturing. *CIRP Journal of Manufacturing Science and Technology* 2(3): 208–215.

Kruth, J.-P., M. Leu, and T. Nakagawa. 1998. Progress in additive manufacturing and rapid prototyping. *Annals of the ClRP* 47(2): 525–540.

Le Bourhis, F., O. Kerbrat, J.-Y. Hascoet, and P. Mognol. 2013. Sustainable manufacturing: Evaluation and modeling of environmental impacts in additive manufacturing. *The International Journal of Advanced Manufacturing Technology* 69(9): 1927–1939.

Levy, G. N., R. Schindel, and J. P. Kruth. 2003. Rapid manufacturing and rapid tooling with layer manufacturing (LM) technologies, state of the art and future perspectives. *CIRP Annals—Manufacturing Technology* 52(2): 589–609.

Lovins, A. B. 1996. Negawatts: Twelve transitions, eight improvements and one distraction. *Energy Policy* 24(4): 331–343.

Maxwell, D. and R. van der Vorst. 2003. Developing sustainable products and services. *Journal of Cleaner Production* 11(8): 883–895.

Mazzioli, A., M. Germani, and R. Raffaeli. 2009. Direct fabrication through electron beam melting technology of custom cranial implants designed in a PHANToM-based haptic environment. *Materials and Design* 30(8): 3186–3192.

Mognol, P., D. Lepicart, and N. Perry. 2006. Rapid prototyping: Energy and environment in the spotlight. *Rapid Prototyping Journal* 12(1): 26–34.

Morrow, W. R., H. Qi, I. Kim, J. Mazumder, and S. J. Skerlos. 2007. Environmental aspects of laser-based and conventional tool and die manufacturing, *Journal of Cleaner Production* 15(10): 932–943.

Murr, L. E., S. M. Gaytan, E. Martinez, F. Medina, and R. B. Wicker. 2012. Next generation orthopaedic implants by additive manufacturing using electron beam melting. *International Journal of Biomaterials* 2012: 1–14.

Murr, L. E., S. A. Quinones, S. M. Gaytan, M. I. Lopez, A. Rodela, E. Y. Martinez, D. H. Hernandez, E. Martinez, F. Medina, and R. B. Wicker. 2009. Microstructure and mechanical behavior of Ti-6Al-4V produced by rapid-layer manufacturing, for biomedical applications. *Journal of the Mechanical Behaviour of Biomedical Materials* 2(1): 20–32.

Psarra, S. and T. Grajewski. 2001. Describing shape and shape complexity using local properties. In Proceedings of the 3rd International Space Syntax Symposium, 7–11 May, Atlanta, GA, USA.

Ruffo, M. and R. Hague. 2007. Cost estimation for rapid manufacturing—Simultaneous production of mixed components using laser sintering. *Proceedings of IMech E Part B: Journal of Engineering Manufacture* 221(11): 1585–1591.

Saidpour, H. 2004. Lightweight high performance materials for car body structures. In NTI Technology Conference, CEME, Ford Motor Company, 16 June, London.

Schaller, R. 1997. Moore's law: Past, present and future. *IEEE Spectrum* 34(6): 53–59.

Spies, K. 1957. Die Zwischenformen beim Gesenkschmieden und ihre Herstellung durch Formwalzen [Intermediate shapes in die forging and their manufacture through roll forming]. Diploma thesis, Technische Hochschule Hannover, Hanover, Germany.

Stoneman, P. 2002. *The economics of technological diffusion*. Oxford, UK: Blackwell.

Strutt, P. R. 1980. A comparative study of electron beam and laser melting of M2 tool steel. *Materials Science and Engineering* 44(2): 239–250.

Taminger, K. M. B. and R. A. Hafley. 2002. Characterization of 2219 aluminium produced by electron beam freeform fabrication. In Solid Freeform Fabrication (SFF) Symposium, 5–7 August, Austin, TX, USA.

Tomov, B. and R. Radev. 2007. Shape complexity factor for closed die forging. In *METAL* 2007, 22–24 May, Hradec nad Moravici, Czech Republic.

Tuck, C. J., R. J. M. Hague, M. Ruffo, M. Ransley, and P. Adams. 2008. Rapid manufacturing facilitated customization. *International Journal of Computer Integrated Manufacturing* 21(3): 245–258.

Vijayaraghavan, A. and D. Dornfeld. 2010. Automated energy monitoring of machine tools. *CIRP Annals—Manufacturing Technology* 59(1): 21–24.

Waldman, M. 2003. Durable goods theory for real world markets. *Journal of Economic Perspectives* 17(1): 131–154.

Westkämper, E., L. Alting, and G. Arndt. 2000. Life cycle management and assessment: Approaches and visions towards sustainable manufacturing (keynote paper). *CIRP Annals—Manufacturing Technology* 49(2): 501–526.

Yokogawa Electric Corporation. 2004. *User's manual IM CW240E*. Tokyo: Yokogawa Electric Corporation.

About the Authors

All authors are members of the 3D Printing Research Group at the Faculty of Engineering at the University of Nottingham, Nottingham, United Kingdom. **Martin Baumers** is a assistant professor, **Chris Tuck** is an associate professor, and **Ricky Wildman**, **Ian Ashcroft**, and **Richard Hague** are professors.

Supporting Information

Additional Supporting Information may be found in the online version of this article at the publisher's web site:

Supporting Information S1: This supporting information documents the pseudocode that expresses the flow and logical structure of the actions performed by a shape complexity measurement algorithm designed to capture the complexity within a succession of 2D shapes built up by Additive Manufacturing in plain English. Note that the pseudocode does not contain function prototypes, variable definitions, and main and function code with correct syntax.